



# Removal of boron from aqueous solution by modified cellulose

Ayşe Gül Yetgin<sup>1</sup> · Ozan Ali Dündar<sup>1</sup> · Emrah Çakmakçı<sup>2</sup> · Özgür Arar<sup>1</sup>

Received: 17 August 2021 / Revised: 6 November 2021 / Accepted: 24 November 2021 / Published online: 4 January 2022  
© The Author(s), under exclusive licence to Springer-Verlag GmbH Germany, part of Springer Nature 2021

## Abstract

Cellulose is a promising alternative material as a sorbent for the removal of pollutants. The availability of hydroxyl groups on cellulose allows for the application of various modification reactions for the development of novel sorbents with different functional groups. In this work, a cellulose sorbent modified with N-methyl-glucamine was prepared and tested for the removal of boron. A batch adsorption process was used to further explore the boron sorption kinetics, isotherms, thermodynamics, mechanism, and reuse of the prepared sorbent. It was found that the optimum sorbent dose for boron removal was 0.2 g/25 mL. Moreover, the initial pH of the solution was found to affect the removal rate and was found to be  $\geq 4$ . The sorption of boron reached equilibrium within 60 min. The maximum sorption capacity was calculated to be 4.7 mg B/g sorbent. The sorption process was found to be exothermic and the negative value of  $\Delta S$  in the range of 30–60 °C is related to a decrease in randomness at the solid/solution interface during the sorption of boron on the sorbent. The sorption/regeneration experiments have shown that the removal rate of the sorbent remains the same over 5 cycles.

**Keywords** Boron · Cellulose · N-Methyl-glucamine · Water treatment

## Nomenclature

$b$	Langmuir constant (L/mg)	$q_e$	Amount of B sorbed onto sorbent at equilibrium (mg/g)
$C_0$	Initial boron concentration in the solution (mg/L)	$q_t$	Amount of B sorbed onto sorbent at any time (mg/g)
$C_e$	Boron concentration in the solution at equilibrium (mg/L)	$r$	Removal efficiency (%)
$k_1$	Pseudo-first-order rate constant ( $\text{min}^{-1}$ )	$R$	Universal gas constant (8.314 J/mol-K)
$k_2$	Pseudo-second-order rate constant (g/mg min)	RE	Regeneration efficiency (%)
$K_F$	Freundlich adsorption constant	$T$	Absolute temperature (K)
$m$	Mass of the sorbent used in the experiment (g)	$t$	Time (min)
$n$	Freundlich adsorption constant	$V$	Volume of solution (L)
$Q_0$	Maximum sorption capacity for Langmuir model (mg/g)	$\Delta G^\circ$	Standard free energy change (kJ/mol)
		$\Delta H^\circ$	Standard enthalpy change (kJ/mol)
		$\Delta S^\circ$	Standard entropy change (kJ/mol K)

✉ Özgür Arar  
ozgur.arar@ege.edu.tr

Ayşe Gül Yetgin  
aysegulyetgin.eu@gmail.com

Ozan Ali Dündar  
ozzy.dundarl1@gmail.com

Emrah Çakmakçı  
emrah.cakmakci@marmara.edu.tr

<sup>1</sup> Faculty of Science, Department of Chemistry, Ege University, 35040 Izmir, Turkey

<sup>2</sup> Chemistry Department, Marmara University, Istanbul, Turkey

## 1 Introduction

Although boron (B) is one of the essential nutrients for humans and plants, it has a toxic effect on plants when present in excessive concentrations [1]. It is normally present in marine and groundwater but its concentration is proportional to the surrounding geology. However, anthropogenic factors also increase its concentration in water [2]. Boric acid is used in a variety of industries including optoelectronics, semiconductors, ceramics and borosilicate glass, B-containing fertilizers, herbicides, and insecticides [3].

The B concentration in such wastes changed from micrograms per liter to milligrams per liter. The concentration of boron in wastewater from hydraulic fracturing was 123 mg/L [4], while in wastewater from liquid crystal displays, it was 820 mg/L [5]. The World Health Organization (WHO) has set 2.4 mg/L as a guideline value for drinking water [6].

The various water treatment techniques such as boron-selective resins, coagulation, membrane processes, and sorption processes used to remove boron and the advantages/limitations of these methods have been studied by various groups [2, 7, 8].

The sorption process is one of the most efficient methods for removing boron at low concentrations. For this purpose, chelating resins, activated carbon, fly ash, and natural materials can be used [9]. The use of low cost, environmentally friendly, and abundant sorbents for water treatment has gained friction. The low cost, biodegradable, renewable, and modifiable properties make cellulose one of the materials with great potential for water treatment [10].

In recent years, various functional groups have been attached to cellulose and then used for contaminant removal. Parlak and Arar [11] used sodium periodate ( $\text{NaIO}_4$ ) and sodium metabisulfite ( $\text{Na}_2\text{S}_2\text{O}_5$ ) successively for the preparation of sulfonated cellulose and then applied it for the removal of copper ( $\text{Cu}^{2+}$ ). The capacity of the sorbent produced was reported to be 8.2 mg  $\text{Cu}^{2+}$ /g. The authors also pointed out that the sorption of  $\text{Cu}^{2+}$  is a fast kinetic and exothermic process [11].

Özdemir et al. [12] applied a two-pot oxidation process for the preparation of diacetate-containing cellulose and tested it for the removal of beryllium ( $\text{Be}^{2+}$ ). Oxidation of cellulose was achieved by sequential oxidation with  $\text{NaIO}_4$  and sodium chlorite ( $\text{NaClO}_2$ ). The sorption of  $\text{Be}^{2+}$  reached equilibrium within 3 min. The capacity of the sorbent was reported to be 4.54 mg/g. The author also reported that 0.1 M HCl or  $\text{H}_2\text{SO}_4$  solutions can be used for the regeneration of the sorbent loaded with Be [12].

Anirudhan et al. [13] prepared quaternary ammonium containing cellulose for the removal of chromium ( $\text{Cr}^{6+}$ ). The removal of  $\text{Cr}^{6+}$  reached equilibrium in 1 h. The capacity of the sorbent was 123.60 mg/g, and the Cr-loaded sorbent was regenerated with 0.1 M NaOH solution [13]. However, to our present knowledge, there is no study on the preparation of N-methyl-glucamine containing cellulose by graft polymerization technique.

Graft polymerization is an attractive method that allows the surface of materials to be functionalized without greatly affecting the properties of the bulk [14]. Graft polymerization, which is used for a variety of applications, has several advantages, such as ease of use, ability to impart different functionalities, tunable surface properties, compatibility and stability, relatively low cost, fast modification rates, and adjustable grafting percentages [14–16]. In our case,

the grafting method allowed us to produce a sorbent with good stability and significantly improved the reusability of the sorbent.

In this work, an N-methyl-glucamine containing sorbent for the removal of boron from an aqueous solution was prepared and investigated. The batch sorption parameters for boron removal were also studied. In addition, the sorption kinetics and sorption capacity of the sorbent as well as the thermodynamic parameters were calculated. In the final phase of the research, the optimum regenerant for the regeneration of the B-loaded sorbent was found.

## 2 Experimental

### 2.1 Chemicals and materials

Glycidyl methacrylate (GMA, 97%, Sigma-Aldrich) and N-methyl-D-glucamine (NMG, 99%, Acros) were used to prepare boron-selective cellulose. The crude cellulose samples were obtained from Denkim Kimya A.Ş. (Denizli, Turkey) and used without pretreatment. The aqueous solution of boric acid was prepared by appropriate dissolution of boric acid ( $\text{H}_3\text{BO}_3$ , Merck) in deionized water.

### 2.2 Preparation of glycidyl methacrylate-N-methyl-D-glucamine monomer

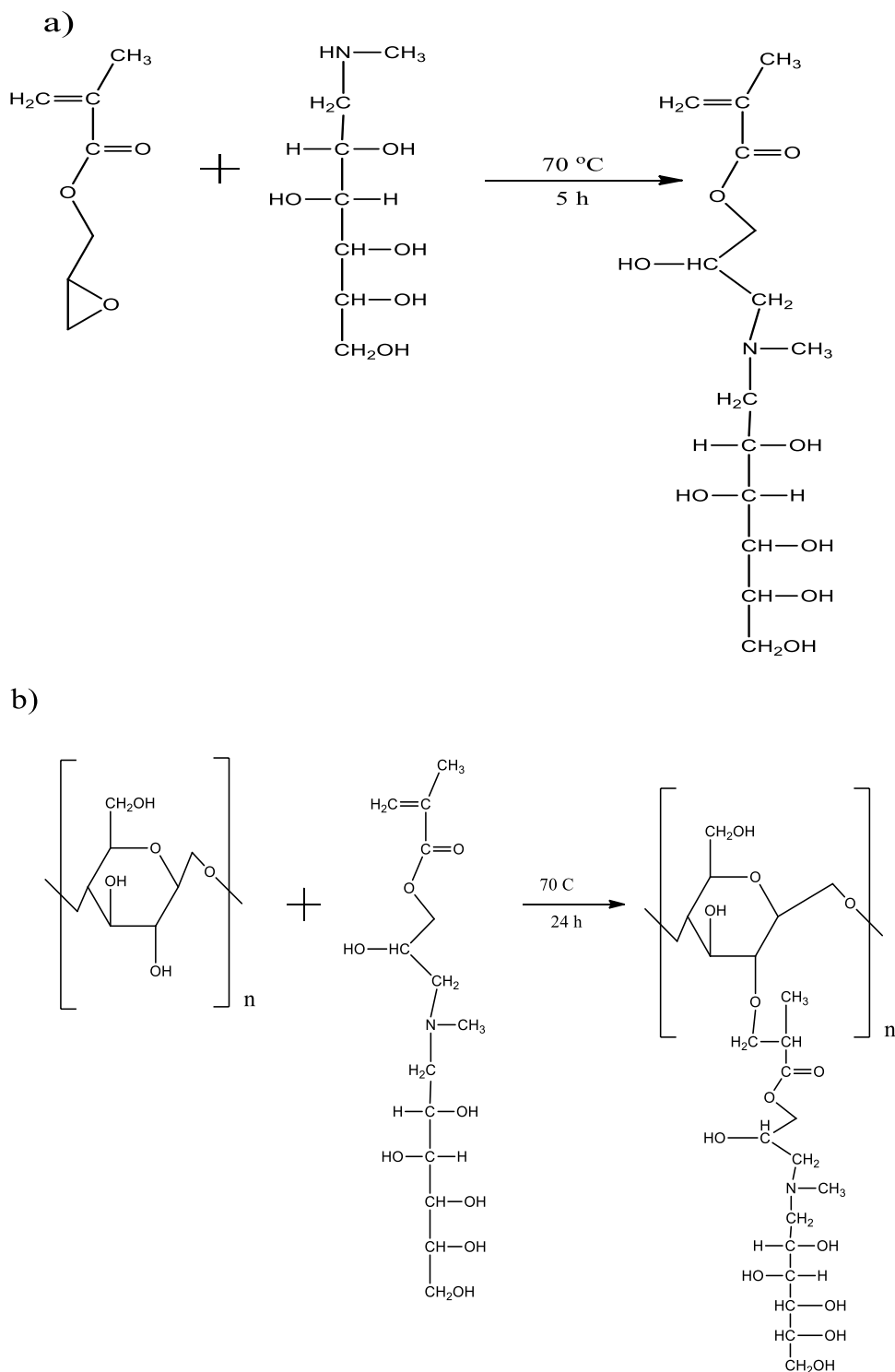
The glycidyl methacrylate-N-methyl-D-glucamine (GMA-NMG) monomer was prepared as described in [17]. Briefly, 150 mL of 0.83 M NMG solution was prepared and added to the reaction cell. Then, 20.4 mL of GMA solution (97%,  $d = 1.042$  g/mL) was slowly added to the NMG solution. The  $\text{N}_2$  gas was passed through the solution for 15 min. The reaction cell was placed in a silicone oil bath at 70 °C for 5 h with vigorous stirring. At the beginning of the process, the mixture was turbid and at the end of the reaction, a single clear phase was observed. The reaction between GMA and NMG is shown in Fig. 1a.

The product was rinsed with diethyl ether (3 times at 50 mL) to remove unreacted GMA. A separatory funnel was used to separate the organic phase from the aqueous phase. The GMA-NMG monomer was in the aqueous phase.

### 2.3 Preparation of GMA-NMG-tethered cellulose

Fifteen grams of crude cellulose and 150 mL of GMA-NMG were added to the reaction cell, and then,  $\text{N}_2$  gas was passed through this mixture. The initiator (0.3366 g  $\text{K}_2\text{S}_2\text{O}_8$ ) was added to the mixture and the reaction cell was placed in an oil bath at 70 °C for 24 h under  $\text{N}_2$  atmosphere to allow the reaction of the hydroxyl groups of cellulose with ethylene

**Fig. 1** Preparation GMA-NMG monomer (**a**) and GMA-NMG-tethered cellulose (**b**)



groups. The reaction of cellulose with GMA-NMG is shown in Fig. 1b.

## 2.4 Characterization of the prepared sorbent

Infrared spectra of crude and GMA-NMG containing cellulose were determined using an infrared spectrometer

(PerkinElmer, model One-B). The elemental composition of the crude and prepared sorbent was determined using an elemental analyzer (Leco, CHNS-932).

The determination of boron in the samples was measured spectrometrically as described in [18].

The removal efficiency ( $r$ ) and capacity ( $q$ ) of the sorbent were calculated according to Eqs. 1 and 2, respectively.

$$q = V \frac{C_0 - C_e}{m} \quad (1)$$

$$r = \frac{C_0 - C_e}{C_0} \times 100 \quad (2)$$

### 3 Results and discussion

#### 3.1 Characterization of the sorbent

The infrared spectrum of raw and modified cellulose is shown in Fig. 2. The peaks at  $3263 \text{ cm}^{-1}$  and  $2924 \text{ cm}^{-1}$  are attributed to the O–H and  $-\text{CH}_3/-\text{CH}_2$  stretching vibrations, respectively. After modification of cellulose, a decrease in this transmittance was observed. The band at  $1713 \text{ cm}^{-1}$  belongs to the C=O bending vibration. Glycidyl methacrylate has C=O groups and the binding of the new C=O groups decreased the transmittance. A new peak appeared at  $1557 \text{ cm}^{-1}$  belonging to amine groups, indicating that GMA-NMG functional groups were successfully attached to cellulose. The peaks at  $1028 \text{ cm}^{-1}$  can be attributed to C–O stretching [11, 12, 19–21].

The elemental composition (carbon C, hydrogen H, nitrogen N, and oxygen O) of crude cellulose was found to be 41.89% C, 6.21% H, and 51.89% O, respectively. The nitrogen (N) was not observed in crude cellulose. In the case of GMA-NMG, the sorbent composition was found to be 44.08% C, 5.31% H, 48.62% O, and 1.99% N. After the introduction of GMA-NMG groups into cellulose, nitrogen was found in the elemental composition, supporting the results of FTIR and further proving the successful grafting of GMA-NMG onto cellulose. It was also observed that the mass fraction of oxygen decreased after modification, which

can be attributed to a lower oxygen mass ratio in the GMA-NMG group.

#### 3.2 Effect of sorbent dose on boron removal

To find the optimal sorbent dose for boron removal, a series of experiments were performed. 25 mL of a boron-containing solution was contacted with different amounts of sorbent (0.1–0.3 g), where the boron concentration in the solution was 5 mg-B/L and the pH of the solution was 6. The variation of boron removal as a function of sorbent dose is shown in Fig. 3.

From Fig. 3, it can be seen that the increase in sorbent dose resulted in an increase in the percentage of boron removal. It is known that the number of available functional groups is linearly proportional to the sorbent dose. When the sorbent dose was increased, the number of functional groups increased and so did the removal rate. Figure 3 also shows that the maximum removal rate was 69% for 0.2 g and further addition of sorbent did not change the removal percentage. Therefore, a sorbent dose of 0.2 g was determined to be the optimum dose and was used in further experiments. Experiments were also conducted with plain cellulose, and as can be seen in Fig. 3, the removal of boron was not observed. These results show that grafting of cellulose improves the removal rate.

#### 3.3 Effect of initial solution pH on boron removal

In this series of experiments, 0.2 g of GMA-NMG-containing cellulose was contacted with 25 mL of boron-containing solution (5 mg-B/L) with different initial pH values of the solution. The results are shown in Fig. 4.

When the pH of the solution was adjusted to 2, 64% of the boron was removed from the solution. Increasing the pH of the solution to 4 increased the boron removal to 69%

**Fig. 2** FTIR spectrum of raw and modified cellulose

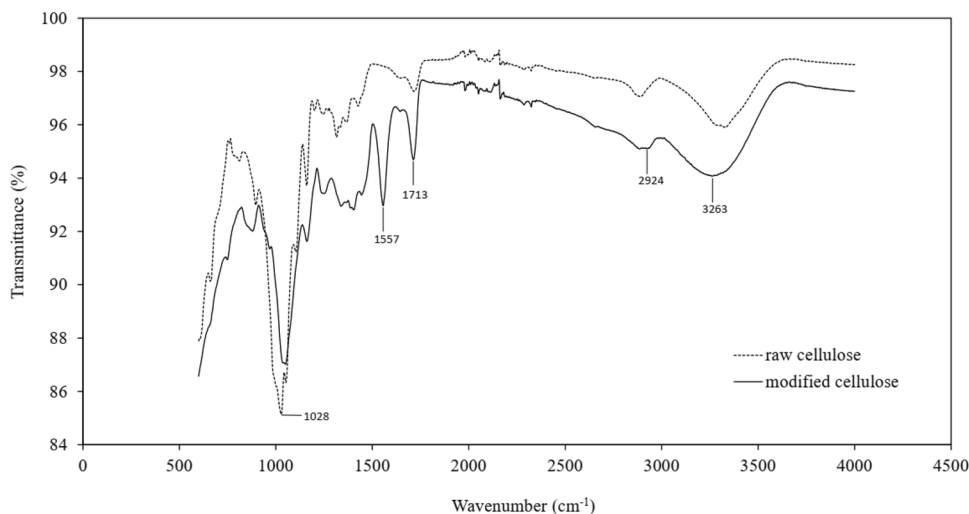


**Fig. 3** Effect of sorbent dose on boron removal

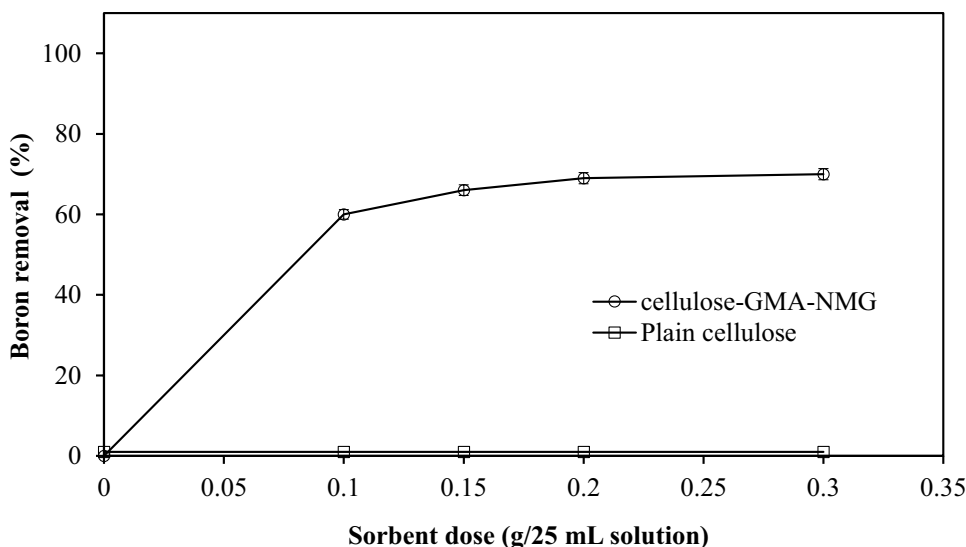
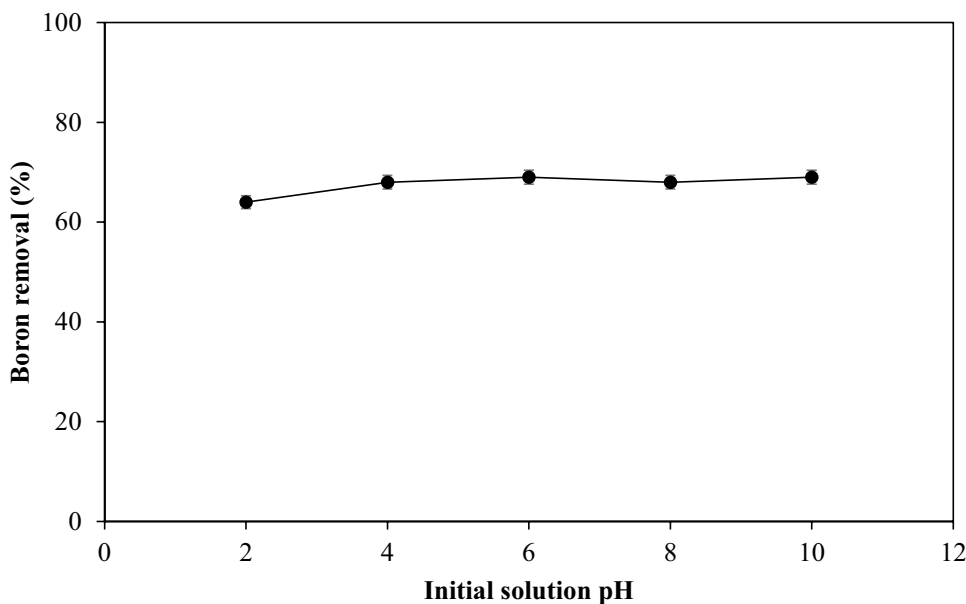
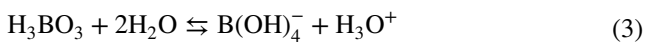


**Fig. 4** Effect of initial solution pH on boron removal



and further increasing the pH to 10 did not change the boron removal rate. The removal of boron by a sorbent containing NMG is a two-step process [22]. First, boric acid dissociates into its anionic form, borate, and hydronium ions (Eq. 3), and in another step, the borate anion forms a chelate with the cis-diol of N-methylglucamine groups, as shown in Fig. 5.



The resulting  $H_3O^+$  ions are sorbed by the ternary amine groups of the NMG [23]. The higher complexability of the N-methyl-D-glucamine group would be an electrostatic attraction between the borate anion and the quaternary ammonium group (after protonation of the ternary amine group of NMG) [24]. When the pH of the solution decreases,

the equilibrium shown in Eq. 3 shifts to the left side, then the molecular form of boric acid occurs and thus the removal of boron decreases.

### 3.4 Sorption kinetics

To find the optimum contact time for boron sorption, 8.0 g of sorbent was contacted with 1.0 L of a B-containing solution (5 mg-B/L, pH 6). The solution was mixed, and 10-mL samples were taken at specific time points. The changes in boron removal versus time are shown in Fig. 6.

As can be seen from Fig. 6, boron sorption reached a plateau after 60 min. The kinetic data are applied to pseudo-first-order (Eq. 4) and pseudo-second-order (Eq. 5) kinetic models [25, 26].

**Fig. 5** Chelation mechanism of boric acid with cis-diol active sites of N-methyl glucamine

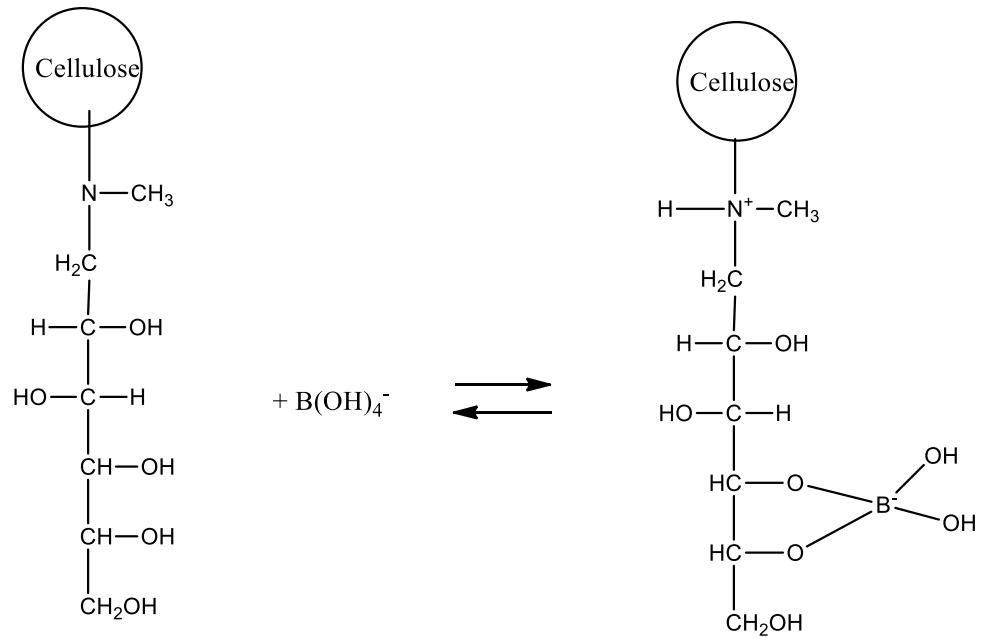
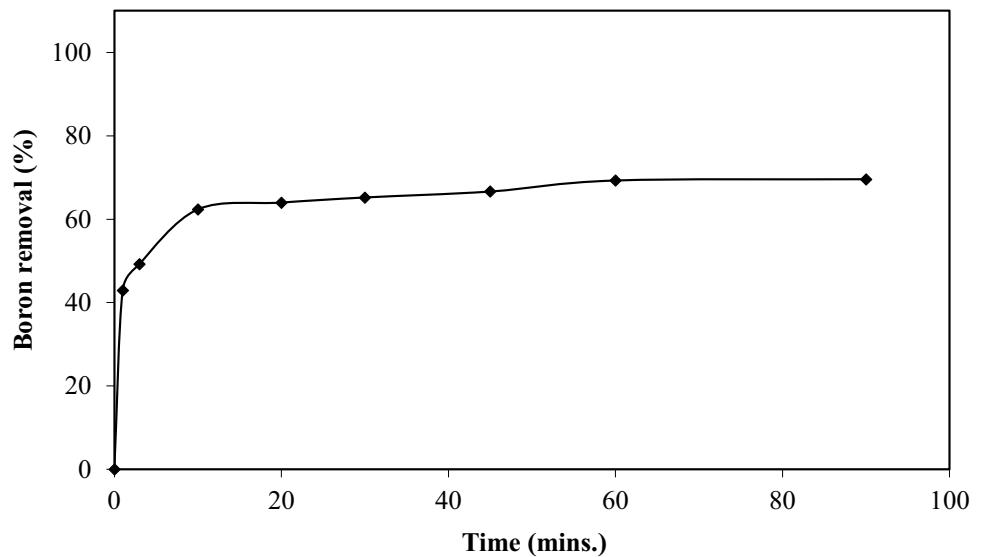


**Fig. 6** Removal of boron versus time



$$\log(q_e - q_t) = \log(q_e) - \frac{k_1 t}{2.303} \quad (4)$$

$$\frac{t}{q_t} = \frac{1}{k_2 q_e^2} + \frac{1}{q_e} t \quad (5)$$

The calculated kinetic data are summarized in Table 1. The regression coefficients ( $R^2$ ) of the pseudo-second-order model were larger than those of the pseudo-first-order model, indicating that the pseudo-second-order kinetic model was more appropriate for the kinetic data obtained.

**Table 1** The calculated parameters of the pseudo-first- and pseudo-second-order kinetic model

Kinetic model	Parameter	value
<b>Pseudo first order</b>	$k_1$ ( $\text{min}^{-1}$ )	0.0285
	$q_e$ (mg/g)	0.0795
	$R^2$	0.8647
<b>Pseudo second order</b>	$k_2$ (g/mg min)	0.2888
	$q_e$ (mg/g)	2.1083
	$R^2$	0.9995

### 3.5 Sorption isotherms

0.2 g of sorbent was contacted with 25 mL of a boron-containing solution. The boron concentration in the solution varied from 25 to 400 mg-B/L (at pH 6). The changes in the capacity of the sorbent compared to the initial boron concentration are shown in Fig. 7. As can be seen in Fig. 7, the sorbent capacity increased with increasing boron concentration, and finally, the sorbent capacity reached its maximum value.

The experimental sorption results are applied to the Langmuir and Freundlich isotherm models. The linear form of the Langmuir model is shown in Eq. 6 and that of the Freundlich model is shown in Eq. 7 [27].

$$\frac{C_e}{Q_e} = \frac{1}{bQ_0} + \frac{C_e}{Q_0} \tag{6}$$

$$\log Q_e = \log K_F + \frac{1}{n} \log C_e \tag{7}$$

The isotherm parameters were calculated and are shown in Table 2. The obtained sorption data showed a better agreement with Langmuir’s isotherm model. This result shows that B sorbed on the prepared sorbent as a monolayer.

The capacity of the sorbent is compared with other sorbents reported in the literature, and the results are summarized in Table 3. The sorbent capacity varied from 0.16 to 199 mg/g. This difference could be due to the type of sorbent, its functional group, modification steps, and composition of the sorbent. For example, a similar work was carried out by Inukai et al. where the authors first modified cellulose with GMA and then further modified the epoxide groups of the grafted GMA

**Table 2** Isotherm model constants and correlation coefficients for the B sorption

Langmuir isotherm constants			Freundlich isotherm constants		
$Q_0$ (mg/g)	$b$ (L/mg)	$R^2$	$K_F$	$n$	$R^2$
4.7136	0.0544	0.9988	1.1177	3.9471	0.9394

with NMG [28]. The authors reported the adsorption capacity of their sorbent as 11.89 mg/g, which is higher than our sorbent. However, their sorbent was tested for only three reuse cycles, and after the second cycle, the recovery percentage decreased to 98%, while in our case, the recovery percentage was almost 100% even after 5 cycles (see Sect. 3.7).

Kamcev et al. have prepared a sorbent containing two NMG functional groups at different locations of the sorbent, which increase the sorption capacity [34]. The use of different starting materials that can bind more than one functional group can increase the removal capacity.

### 3.6 Thermodynamic studies

Thermodynamic studies were performed by varying the solution temperatures (30, 40, 50, and 60 °C). 0.2 g of the sorbent was mixed with 25 mL of boron-containing solution (5 mg-B/L, pH 6).

The changes in standard free energy ( $\Delta G^\circ$ ), entropy ( $\Delta S^\circ$ ), and enthalpy ( $\Delta H^\circ$ ) were estimated using the following Eqs. 8–10 [42].

$$\Delta G = -RT \ln K_d \tag{8}$$

**Fig. 7** Sorption isotherm for prepared sorbent

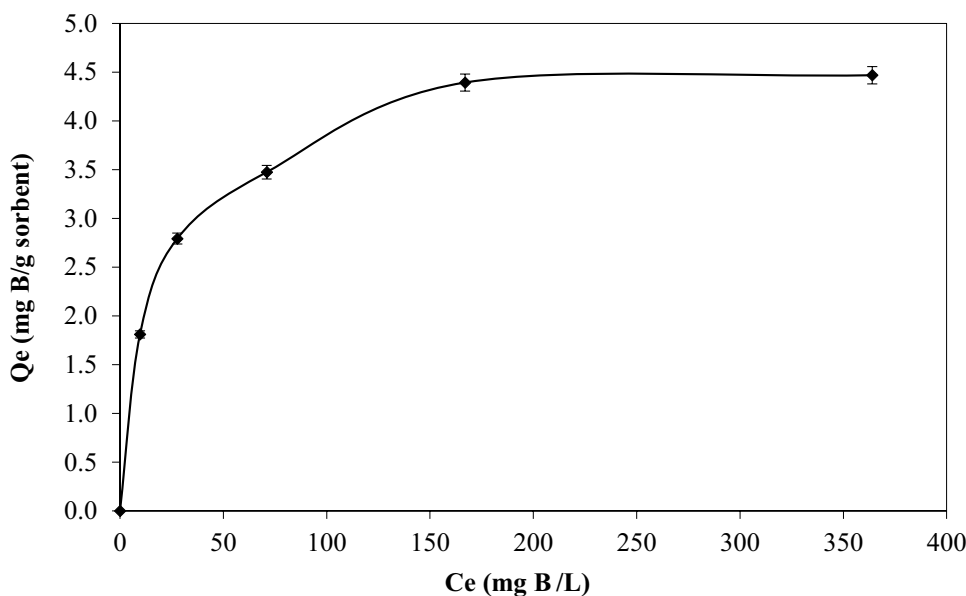


**Table 3** Boron sorption capacities of different sorbents

Sorbent	Maximum sorption capacity (mg/g)	Temperature (°C)	References
Calcined alunite	3.39	25	[29]
Magnesite and bentonite clay composite	4	-	[30]
Calcium alginate gel beads	199	20	[31]
Neutralized red mud	30.12	25	[32]
Mg-Fe hydrotalcite	3.6	25	[33]
Mg-Al hydrotalcite	14		
Porous aromatic framework PAF-1-NMDG	18.38	25	[34]
Porous aromatic framework P2-NMDG	10.87		
Chelest Fiber GRY-HW fiber	18.52	25	[35]
Diaion CRB02 boron-selective resin	13.18		
Diaion CRB05 boron-selective resin	17.45		
Cellulose-based microsphere	12.4	25	[36]
Functionalized polyacrylonitrile	5.5	25	[37]
Fly ash agglomerates	0.16	25	[38]
Ionic liquid loaded cellulose nanocrystals	89.4	25	[39]
Powder cellulose-NMG	11.89	-	[28]
Fiber cellulose-NMG	11.89		
polyethylene (PE) non-woven fiber-NMG		-	[40]
Cellulose acetate-ribose	17.6	25	[41]
Cellulose acetate-NMG	32.4		
Cellulose-GMA-NMG	4.71	25	This work

$$\ln K_d = \frac{\Delta S^\circ}{R} - \frac{\Delta H^\circ}{RT} \quad (9)$$

$$\Delta G^\circ = \Delta H^\circ - T\Delta S^\circ \quad (10)$$

The calculated enthalpy change ( $\Delta H^\circ$ ) was found as  $-25.87$  kJ/mol. The negative values indicate that the sorption phenomena are exothermic. The entropy change was ( $\Delta S^\circ$ )  $-0.097$  kJ/mol K, which means the loss of vibrational and rotational freedom of the groups of OH in GMA-NMG was involved in complexation with the boron atom [43]. The calculated values of standard free energy change ( $\Delta G^\circ$ ) were positive for all temperature changes, implying that the extent of sorption is limited [44]. This could be due to the complexation of boron especially with cis-diol groups.

### 3.7 Regeneration and reuse of the sorbent

The regeneration process for the exhausted sorbent is the same as explained elsewhere [11]. The regeneration efficiency (RE, %) was calculated according to Eq. 11. The results are presented in Table 4. The results show that the sorbent can be regenerated with 0.5 M HCl or 0.5 M  $H_2SO_4$  with efficiency more than 99%

$$RE(\%) = \frac{\text{desorbed amount of B from sorbent (mg)}}{\text{sorbed amount of B on sorbent (mg)}} \times 100 \quad (11)$$

**Table 4** Regeneration performance of different eluent

Regenerant	Regeneration efficiency (%)
0.1 M HCl	98
0.5 M HCl	> 99
0.1 M $H_2SO_4$	> 99
0.5 M $H_2SO_4$	> 99

The desorption and reuse tests of the prepared sorbent were carried out. In this part of the experiments, the 0.2 g sorbent was contacted with 25 mL of a boron-containing solution (5 mgB/L) for 1 h; then, the sorbent was removed from the solution and washed with deionized water. Regeneration of the sorbent was performed with 0.5 M 25 mL  $H_2SO_4$  solution. The sorbent was kept in contact with the  $H_2SO_4$  solution for 1 h. Then, it was removed from the acidic solution and washed with NaOH solution (pH 12) to remove the excess of  $H_2SO_4$  from the sorbent and convert the quaternary groups to the free base form. After washing with NaOH solution, the sorbent was washed with deionized water to remove excess alkali from the sorbent and then used for further sorption tests. The sorption regeneration performance of the sorbent is shown in Fig. 8. As can be seen from the figure, the performance of the sorbent did not change after 5 sorption cycles, which can be considered a promising advantage from the environmental and economic point of view.



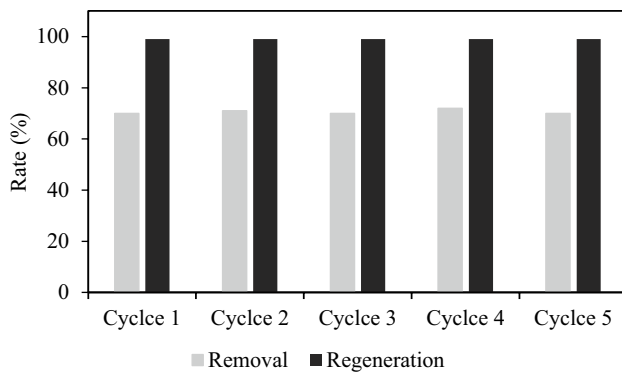


**Fig. 8** Removal and regeneration rate of cycle test

## 4 Conclusions

In summary, cellulose containing N-methyl-glucamine was prepared by a two-step process. In the first step, the glycidyl methacrylate-N-methyl glucamine monomer was synthesized, and in the second step, the monomer was attached to the cellulose. FTIR and elemental analysis confirmed the successful preparation of the sorbent. The results showed that optimal boron removal can be achieved at  $\text{pH} \geq 4$ . The sorption reached equilibrium in 60 min. The maximum sorption capacity was found to be 4.7 mg B/g sorbent. Thermodynamic studies showed that the sorption of boron is exothermic and followed by a decrease in the randomness of the system. More than 99% of boron was desorbed during the regeneration process, and the sorbent can be used for at least five adsorption–desorption cycles.

**Acknowledgements** The authors thank Denkim Kimya A.Ş. for providing the cellulose samples. The authors also thank Dr. Emre Seyyal for his valuable comments on this paper and proofreading the manuscript.

**Funding** This study is supported by Ege University Scientific Research Projects Coordination Unit (Project Number: FLP-2020–22167). Ege Üniversitesi, FLP-2020–22167, Özgür Arar

**Data availability** All data generated or analyzed during this study are included in this published article.

## References

- Chen M, Dollar O, Shafer-Peltier K et al (2020) Boron removal by electrocoagulation: removal mechanism, adsorption models and factors influencing removal. *Water Res* 170:115362. <https://doi.org/10.1016/j.watres.2019.115362>
- Lin J-Y, Mahasti NNN, Huang Y-H (2021) Recent advances in adsorption and coagulation for boron removal from wastewater: a comprehensive review. *J Hazard Mater* 407:124401. <https://doi.org/10.1016/j.jhazmat.2020.124401>
- Hasenmueller EA, Criss RE (2013) Multiple sources of boron in urban surface waters and groundwaters. *Sci Total Environ* 447:235–247. <https://doi.org/10.1016/j.scitotenv.2013.01.001>
- Sari MA, Chellam S (2015) Mechanisms of boron removal from hydraulic fracturing wastewater by aluminum electrocoagulation. *J Colloid Interface Sci* 458:103–111. <https://doi.org/10.1016/j.jcis.2015.07.035>
- Mohapatra D, Chaudhury GR, Park KH (2008) Solvent extraction approach to recover boron from wastewater generated by the LCD manufacturing industry: part 1. Mining, Metall Explor 25:175–180. <https://doi.org/10.1007/BF03403405>
- Guidelines for drinking-water quality WHO (2003) Boron in drinking-water background. *Health criteria other Support Inf* 2:1–17
- Wolska J, Bryjak M (2013) Methods for boron removal from aqueous solutions — a review. *Desalination* 310:18–24. <https://doi.org/10.1016/j.desal.2012.08.003>
- Güler E, Kaya C, Kabay N, Arda M (2015) Boron removal from seawater: state-of-the-art review. *Desalination* 356:85–93. <https://doi.org/10.1016/j.desal.2014.10.009>
- Guan Z, Lv J, Bai P, Guo X (2016) Boron removal from aqueous solutions by adsorption — a review. *Desalination* 383:29–37. <https://doi.org/10.1016/j.desal.2015.12.026>
- Qin F, Fang Z, Zhou J et al (2019) Efficient removal of  $\text{Cu}^{2+}$  in water by carboxymethylated cellulose nanofibrils: performance and mechanism. *Biomacromol* 20:4466–4475. <https://doi.org/10.1021/acs.biomac.9b01198>
- Parlak E, Arar Ö (2018) Removal of copper ( $\text{Cu}^{2+}$ ) from water by sulfonated cellulose. *J Dispers Sci Technol* 39:1403–1408. <https://doi.org/10.1080/01932691.2017.1405818>
- Özdemir VT, Tuğaç HM, Arar Ö (2020) Two-pot oxidative preparation of dicarboxylic acid containing cellulose for the removal of Beryllium ( $\text{Be}^{2+}$ ) from aqueous solution. *Curr Anal Chem* 16:.. <https://doi.org/10.2174/1573411016999200719232310>
- Anirudhan TS, Nima J, Divya PL (2013) Adsorption of chromium(VI) from aqueous solutions by glycidylmethacrylate-grafted-densified cellulose with quaternary ammonium groups. *Appl Surf Sci* 279:441–449. <https://doi.org/10.1016/j.apsusc.2013.04.134>
- Bhattacharya A (2004) Grafting: a versatile means to modify polymers: techniques, factors and applications. *Prog Polym Sci* 29:767–814. <https://doi.org/10.1016/j.progpolymsci.2004.05.002>
- Gowda DV, Koshy T, Godugu K, Srivastava A (2016) Polymer grafting—an overview. *Am J Pharmatech Res* 6:1–13
- Wang S, Wang Z, Li J et al (2020) Surface-grafting polymers: from chemistry to organic electronics. *Mater Chem Front* 4:692–714. <https://doi.org/10.1039/C9QM00450E>
- Arar O, Kabay N, Sánchez J et al (2014) Removal of arsenic from water by combination of electro-oxidation and polymer enhanced ultrafiltration. *Environ Prog Sustain Energy* 33:918–924. <https://doi.org/10.1002/ep.11876>
- Holdich RG, Cumming IW, Perni S (2006) Boron mass transfer during seeded microfiltration. *Chem Eng Res Des* 84:60–68. <https://doi.org/10.1205/cherd.05015>
- Abdul Razak S, Mahadi AH, Abdullah R et al (2020) Biohydrogen production from photodecomposition of various cellulosic biomass wastes using metal-TiO<sub>2</sub> catalysts. *Biomass Convers Biorefinery*. <https://doi.org/10.1007/s13399-020-01164-4>
- Arar Ö (2020) Co-precipitative preparation of a sulfonated cellulose-magnetite hybrid sorbent for the removal of  $\text{Cu}^{2+}$  Ions. *Anal Sci* 36:81–86. <https://doi.org/10.2116/analsci.19SAP01>
- Puri S, Sharma S, Kumari A et al (2020) Extraction of lignocellulosic constituents from cow dung: preparation and characterisation of nanocellulose. *Biomass Convers Biorefinery*. <https://doi.org/10.1007/s13399-020-01119-9>
- Sarıçipek EN, Tuğaç MM, Özdemir VT et al (2021) Removal of boron by boron selective resin-filled electrodeionization. *Environ*

- Technol Innov 23:101742. <https://doi.org/10.1016/j.eti.2021.101742>
23. Kabay N, Sarp S, Yuksel M et al (2007) Removal of boron from seawater by selective ion exchange resins. *React Funct Polym* 67:1643–1650. <https://doi.org/10.1016/j.reactfunctpolym.2007.07.033>
  24. Yoshimura K, Miyazaki Y, Ota F et al (1998) Complexation of boric acid with the N-methyl-D-glucamine group in solution and in crosslinked polymer. *J Chem Soc Faraday Trans* 94:683–689. <https://doi.org/10.1039/a707790d>
  25. Ho Y, McKay G (1999) Pseudo-second order model for sorption processes. *Process Biochem* 34:451–465. [https://doi.org/10.1016/S0032-9592\(98\)00112-5](https://doi.org/10.1016/S0032-9592(98)00112-5)
  26. Ho Y, McKay G (1998) Sorption of dye from aqueous solution by peat. *Chem Eng J* 70:115–124. [https://doi.org/10.1016/S1385-8947\(98\)00076-X](https://doi.org/10.1016/S1385-8947(98)00076-X)
  27. Alyüz B, Veli S (2009) Kinetics and equilibrium studies for the removal of nickel and zinc from aqueous solutions by ion exchange resins. *J Hazard Mater* 167:482–488. <https://doi.org/10.1016/j.jhazmat.2009.01.006>
  28. Inukai Y, Tanaka Y, Matsuda T et al (2004) Removal of boron(III) by N-methylglucamine-type cellulose derivatives with higher adsorption rate. *Anal Chim Acta* 511:261–265. <https://doi.org/10.1016/j.aca.2004.01.054>
  29. Kavak D (2009) Removal of boron from aqueous solutions by batch adsorption on calcined alunite using experimental design. *J Hazard Mater* 163:308–314. <https://doi.org/10.1016/j.jhazmat.2008.06.093>
  30. Masindi V, Gitari MW, Tutu H, Debeer M (2016) Removal of boron from aqueous solution using magnesite and bentonite clay composite. *Desalin Water Treat* 57:8754–8764. <https://doi.org/10.1080/19443994.2015.1025849>
  31. Ruiz M, Tobalina C, Demey-Cedeño H et al (2013) Sorption of boron on calcium alginate gel beads. *React Funct Polym* 73:653–657. <https://doi.org/10.1016/j.reactfunctpolym.2013.01.014>
  32. Cengeloglu Y, Tor A, Arslan G et al (2007) Removal of boron from aqueous solution by using neutralized red mud. *J Hazard Mater* 142:412–417. <https://doi.org/10.1016/j.jhazmat.2006.08.037>
  33. Ferreira OP, de Moraes SG, Durán N et al (2006) Evaluation of boron removal from water by hydrotalcite-like compounds. *Chemosphere* 62:80–88. <https://doi.org/10.1016/j.chemosphere.2005.04.009>
  34. Kamcev J, Taylor MK, Shin D et al (2019) Functionalized porous aromatic frameworks as high-performance adsorbents for the rapid removal of boric acid from water. *Adv Mater* 31:1808027. <https://doi.org/10.1002/adma.201808027>
  35. Recepoğlu YK, Kabay N, Yılmaz-İpek İ et al (2017) Deboronation of geothermal water using N-methyl-D-glucamine based chelating resins and a novel fiber adsorbent: batch and column studies. *J Chem Technol Biotechnol* 92:1540–1547. <https://doi.org/10.1002/jctb.5234>
  36. Liu S, Xu M, Yu T et al (2017) Radiation synthesis and performance of novel cellulose-based microsphere adsorbents for efficient removal of boron (III). *Carbohydr Polym* 174:273–281. <https://doi.org/10.1016/j.carbpol.2017.06.012>
  37. Wang J, Wang T, Li L et al (2014) Functionalization of polyacrylonitrile nanofiber using ATRP method for boric acid removal from aqueous solution. *J Water Process Eng* 3:98–104. <https://doi.org/10.1016/j.jwpe.2014.05.015>
  38. Polowczyk I, Ulatowska J, Koźlecki T et al (2013) Studies on removal of boron from aqueous solution by fly ash agglomerates. *Desalination* 310:93–101. <https://doi.org/10.1016/j.desal.2012.09.033>
  39. Wahib SA, Da'na DA, Ashfaq MY, Al-Ghouti MA (2021) Functionalized cellulose nanocrystals as a novel adsorption material for removal of boron from water. *Case Stud Chem Environ Eng* 4:100121. <https://doi.org/10.1016/j.cscee.2021.100121>
  40. Ting T-M, Hoshina H, Seko N, Tamada M (2013) Removal of boron by boron-selective adsorbent prepared using radiation induced grafting technique. *Desalin Water Treat* 51:2602–2608. <https://doi.org/10.1080/19443994.2012.749054>
  41. Hong M, Li D, Wang B et al (2021) Cellulose-derived polyols as high-capacity adsorbents for rapid boron and organic pollutants removal from water. *J Hazard Mater* 419:126503. <https://doi.org/10.1016/j.jhazmat.2021.126503>
  42. Babu DK, Ravindhranath K, Mekala S (2021) Simple effective new bio-adsorbents for the removal of highly toxic nitrite ions from wastewater. *Biomass Convers Biorefinery*. <https://doi.org/10.1007/s13399-021-01677-6>
  43. Dawber JG, Matusin DH (1982) Potentiometric and polarimetric studies of the reaction of boric acid and tetrahydroxyborate ion with polyhydroxy compounds. *J Chem Soc Faraday Trans 1 Phys Chem Condens Phases* 78:2521. <https://doi.org/10.1039/f19827802521>
  44. Shahwan T (2021) Critical insights into the limitations and interpretations of the determination of  $\Delta G^\circ$ ,  $\Delta H^\circ$ , and  $\Delta S^\circ$  of sorption of aqueous pollutants on different sorbents. *Colloid Interface Sci Commun* 41:100369. <https://doi.org/10.1016/j.colcom.2021.100369>

**Publisher's note** Springer Nature remains neutral with regard to jurisdictional claims in published maps and institutional affiliations.